Effect of V Dopant on Physicochemical Properties of Vanadium-Doped Anatase Synthesized via Simple Reflux Technique

Hari Sutrisno[1], Ariswan[2] & Dyah Purwaningsih[1]

[1] Department of Chemistry Education, Faculty of Mathematics and Natural Sciences, Yogyakarta State University, Kampus Karangmalang, Jl. Colombo 1, Yogyakarta, 55281, Indonesia
[2] Department of Physics Education, Faculty of Mathematics and Natural Sciences, Yogyakarta State University, Kampus Karangmalang, Jl. Colombo 1, Yogyakarta, 55281, Indonesia
Email: sutrisnohari@uny.ac.id

Abstract. Mesoporous pure TiO_2 (M-TiO_2) and mesoporous-vanadium-doped TiO_2 (M-V-doped TiO_2) were successfully synthesized via a facile and simple reflux technique. The purpose of this research was to study the effect of vanadium dopant on the physicochemical properties of all materials obtained. Characterization of the prepared materials was carried out using X-ray diffraction (XRD), scanning electron microscopy-energy dispersive X-ray spectroscopy (SEM-EDS) and N_2-adsorption-desorption analysis. The presence of Ti and O elements in M-TiO_2 and of Ti, V and O elements in M-V doped TiO_2 could be detected by SEM-EDS, while the patterns of X-ray diffraction of all the prepared samples had a well-crystalline surface of anatase type. All mesoporous vanadium-doped TiO_2 (M-V-doped TiO_2) materials performed in a highly transparent mode in the visible region at 554 nm (E_g = 2.24 eV) and 588 nm (E_g = 2.12 eV) for 3.3 and 4.9 wt% V doped TiO_2, respectively. The Rietveld refinement method was applied to extract the structural parameters of the M-TiO_2 and M-V-doped TiO_2 using the Fullprof program in the WinPlotr package. The prepared materials were refined in the crystal system and space group of anatase (tetragonal, $I4_1/amd$ (141)). The vanadium ion was successfully doped into TiO_2. The isotherm type of M-TiO_2 and 2.3 wt% V doped TiO_2 were of type IV, with a profile of type H2 hysteresis loops, while the 3.3 and 4.9 wt% vanadium-doped TiO_2 reflected isotherm type III. The Brunauer-Emmett-Teller (BET) results showed a significant reduction in surface area due to increased concentrations of vanadium. The highest values of BET-specific surface area, pore volume and average pore size of M-TiO_2 were 46 m^2/g, 18.45 nm and 0.2572 cm^3/g respectively.

Keywords: *anatase; hysteresis; mesoporous materials; reflux technique; Rietveld analysis.*

1 Introduction

Titanium dioxide or titania (TiO_2) is an n-type semiconductor that has a wide band-gap with specific chemical properties and stability. TiO_2 has attracted a great deal of interest over the past decades due to its special physiochemical properties. A

Received August 4th, 2015, 1st Revision December 5th, 2015, 2nd Revision March 4th, 2016, 3rd Revision March 13th, 2016, Accepted for publication March 14th, 2016.
 ISSN: 2337-5760, DOI: 10.5614/j.math.fund.sci.2016.48.1.8

number of potential applications of TiO_2 in both fundamental research and practical development work, have been developed, including in photocatalysis [1,2], photovoltaic cells [3,4], photoinduced super-hydrophilicity [5,6] and anti-bacterial applications [7,8].

The properties of TiO_2 depend on the phase, surface area, dopant, degree of crystallization, particle size, pore size and morphology. For TiO_2 photocatalysis and photoinduced super-hydrophilicity, efforts have been made in two aspects: the first is to narrow the wide band gap semiconductor of TiO_2 to extend the spectral response to the visible region or ultra violet radiation, among others by doping with nonmetallic dopants such as N [9], C [10] and S [11]. The other is to minimize the recombination rate of the photogenerated electron-hole pairs by doping with transition metals such as Ag [12,13], V [14] and Cr [15] into TiO_2 to develop visible-photocatalysts. Among transition metal ions, vanadium ion is attractive as dopant because it will generate an intermediate band so that absorption will happen in the visible region. Various methods have been selected to prepare V doped doped TiO_2 photocatalysts, such as a hydrothermal method [16], electro spinning technique [17], wet chemical method [14,18], sol-gel method [19,20], flame spray pyrolysis technique [21], and anodic oxidation [22].

In this study, pure and 2.3, 3.3, 4.9 wt% V doped mesoporous-TiO_2 were prepared by reflux technique at 150 °C for 6 hours. Mesoporous material can be synthesized by using templates, for example surfactant, lipid, polymer etc. and free-templates. This research synthesized pure and V-doped TiO_2 mesoporous materials without using a template. In previous studies, mesoporous materials were produced with free templates at low temperatures, for example by hydrothermal and solvothermal methods [23,24]. At low temperatures, the polycondensation process takes place very slowly, especially propagation, which consists of olation and oxolation that allow to control the formation of pores, the crystal structure and morphology [25]. The morphology and the influence of V doped-TiO_2 were investigated using scanning electron microscopy (SEM) and energy dispersive X-ray spectroscopy (EDS), respectively. The purpose of the research was to observe the role of the V dopants with respect to their physicochemical properties.

2 Experiment

2.1 Materials

Ammonium hydroxide (NH_4OH, 28-30% NH_3 basis) solution, hydrogen peroxide solution (H_2O_2, 10 wt. % in H_2O), ammonium metavanadate (NH_4VO_3, 99%), titanium (IV) chloride ($TiCl_4$, 99%) manufactured by Sigma-Aldrich were purchased. All the reagents were used without purification. $Ti(O_2)O.2H_2O$ was obtained from the reaction of $TiCl_4$ and H_2O_2 [26]. In a typical procedure, 50 ml of

$TiCl_4$ was added into a 500 ml glass flask loaded in an ice water bath and then 25 ml of H_2O_2 was added slowly into the reaction vessel under magnetic stirring.

2.2 Preparation of M-TiO_2 and M-V doped TiO_2

A series of vanadium doped TiO_2 at various weight percentages of V doped TiO_2 was prepared by reflux technique. Mesoporous-TiO_2 (M-TiO_2) and mesoporous-vanadium-doped TiO_2 (M-V doped TiO_2) were prepared. In a typical synthesis, 10 g $Ti(O_2)O.2H_2O$ was dissolved in 50 ml of distilled water under vigorous stirring. The solution was stirred for 4 hours to obtain a colloidal A. To determine the effect of the NH_4VO_3 concentration, 0, 3, 6 and 9 wt% V doped TiO_2 respectively were adopted in a separated beaker. The samples were thoroughly dissolved in 20 mL of distilled water under vigorous stirring to obtain solution B1, B2, B3, and B4 respectively. Each B1, B2, B3 and B4 colloid was then slowly added to each colloid A. The four types of final solution mixtures were sealed and further stirred for 2 h, after which NH_4OH was added dropwise until the pH value reached about 8-10. Finally, the solution mixtures were heated with a magnetic stirrer in reflux equipment at 150°C for 6 hours. The obtained precipitate was filtered, washed with distilled water and dried at 70°C for 3 hours. Finally, the precipitate materials were calcined at 600°C for 2 hours.

2.3 Characterization

The morphologies were characterized using a Phenom ProX Desktop scanning electron microscope (SEM). The influence of the vanadium load on the structural characteristics of the vanadium-doped TiO_2 and the presence of Ti, V and O elements in the prepared materials were analyzed using energy dispersive X-ray spectroscopy (EDS).

All samples were suspensed in ethanol solution. The colloidal samples were evaluated using a Shimadzu 2450 UV-vis diode array spectrophotometer.

The prepared materials were examined using powder X-ray diffraction (XRD). The XRD patterns were obtained on a Rigaku Miniflex 600-Benchtop XRD instrument, operated in the Bragg configuration using Cu Kα radiation (λ = 1.5406 Å). The XRD instrument was run at 40 kV and 15 mA. The XRD data were collected in steps of 0.02° with a count time of 15 s/step. The intensities were determined in the 2Θ interval ranging from 20° to 90°. To refine the crystal structures from the powder diffraction data, the Rietveld analysis was carried out using the Fullprof program by Roisnel and Rodriguez Carbajal in the WinPlotr package [27]. The following parameters were refined: unit cell, scale factor, and full width at half-maximum (FWHM).

The conventional analysis of N_2 adsorption-desorption isotherms was carried out at 77 K with a Micromeritics ASAP 2020 instrument based on adsorption-desorption

data (55 points). The samples were degassed at 150 °C under vacuum for 4 h prior to analysis with a vacuum set point of 10 μmHg. The Brunauer-Emmett-Teller (BET) specific surface area (S_{BET}) data were collected based on adsorption data (10 point) in the multi-point BET measurement from (P/P0) of ~ 0.06 to ~ 0.30 [28]. The pore volume and average pore size were evaluated from the adsorption-desorption isotherms by the procedure developed by Barrett, Joyner and Halenda (BJH) [29]. The BET and BJH calculations were done with the ASAP 2020 V4.01 software from Micromeritics.

3 Results and Discussions

3.1 SEM images and EDS analysis

Typical SEM images and EDS analysis of M-TiO_2 and M-V doped doped TiO_2 nanocrystalline are shown in Figure 1. Figures 1(a)-1(d) show that the particles were highly agglomerated.

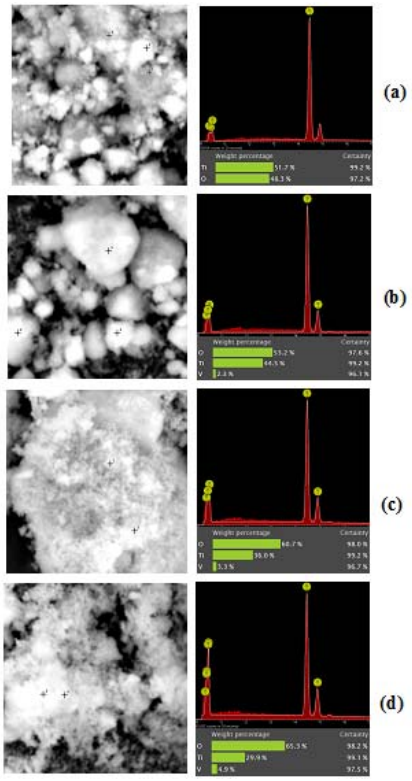

Figure 1 SEM images, EDS analysis and weight percentage (%) of Ti, O and V in M-TiO_2 (a), 2.3 wt% V doped TiO_2 (b), 3.3 wt% V doped TiO_2 (c), and 4.9 wt% V doped TiO_2(d).

The EDS analysis identified the presence of Ti and O elements in the M-TiO_2 and the presence of Ti, V and O elements in the M-V doped TiO_2. As shown in Figure 1, the increasing concentration of NH_4VO_3 also increased the quantity of V in the M-V doped TiO_2. The crystal of V_2O_5 was found in the 4.9 wt% V doped TiO_2, which was confirmed by the XRD pattern (Figure 2(d)). Table 1 shows that the addition of 3, 6 and 9 wt% V doped TiO_2 produced only 2.3, 3.3 and 4.9 wt% V doped TiO_2 respectively.

Table 1 Weight percentage of Ti, O and V of M-TiO_2 and M-V Doped TiO_2.

Samples	Weight Percentage (wt%)			Mole ratio = Ti:V
	Ti	V	O	
Pure TiO_2	51.7	0	48.3	1.079 : 0.000
2.3 wt% V doped TiO_2	44.5	2.3	53.2	0.958 : 0.040
3.3 wt% V doped TiO_2	36.0	3.3	60.7	0.922 : 0.074
4.9 wt% V doped TiO_2	29.9	4.9	65.3	0.868 : 0.126

3.2 Optical Properties

In order to investigate the optical properties of the M-TiO_2 and M-V doped TiO_2 samples at 2.3, 3.3 and 4.9 wt% V doped TiO_2, the absorbance was measured as a function of wavelength in the range of 200-800 nm. The UV-visible spectra for the M-V doped TiO_2 samples at 2.3, 3.3 and 4.9 wt% V doped TiO_2 are shown in Figure 2. For comparison purposes, the spectrum of undoped TiO_2 (M-TiO_2) is also displayed. All mesoporous V-doped TiO_2 (M-V doped TiO_2) powders performed in a highly transparent mode in the visible region at 554 nm (E_g = 2.24 eV) and 588 nm (E_g = 2.12 eV) for the 3.3 and 4.9 wt% V doped TiO_2, respectively.

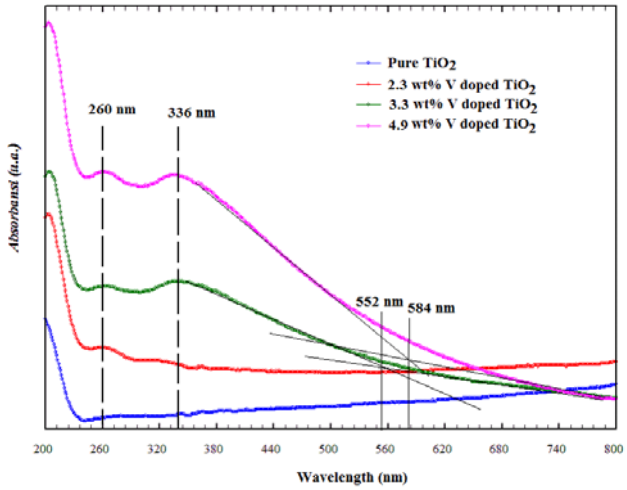

Figure 2 UV-Vis spectra of undoped TiO_2 and M-V doped TiO_2 at 2.3, 3.3 and 4.9 wt% V doped TiO_2 suspensed in ethanol solution.

3.3 XRD Analysis

The wide-angle XRD patterns of the M-TiO_2 and the M-V doped TiO_2 are presented in Figure 3. The peak positions at 2θ: 25.36, 37.04, 37.88, 38.61, 48.11, 53.96, 55.10, 62.11, 62.69, 68.75, 70.26, 75.01, 75.96, and 82.65° are in accordance with the TiO_2 anatase phase. The main diffraction peaks can be indexed as the (101), (103), (004), (112), (200), (105), (211), (213), (204), (116), (220), (215), (301), and (224) reflections of anatase crystalline phase matching as shown in JCPDS card No. 21-1272. The reflections of TiO_2(B) phase can be observed in the prepared M-TiO_2. The presence of TiO_2(B) phase is characterized by the presence of diffraction peaks at 2θ = 30.7° [30].

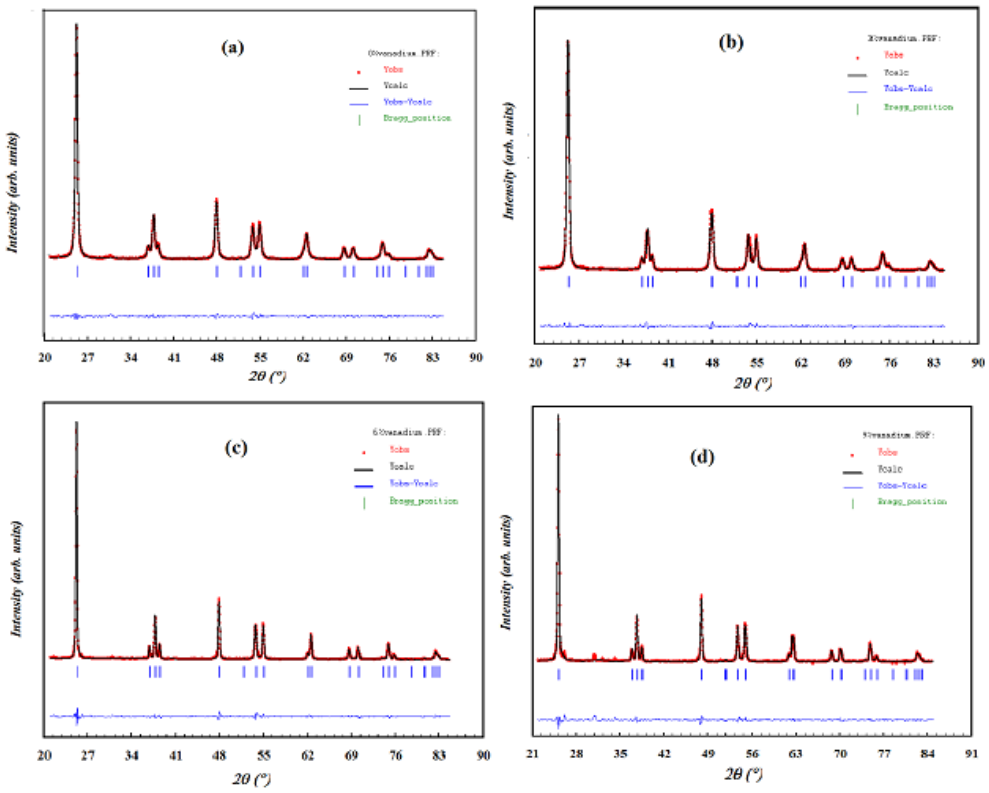

Figure 3 Rietveld refinement patterns of M-TiO_2 (a), 2.3 wt% V doped TiO_2 (b), 3.3 wt% V doped TiO_2 (c), and 4.9 wt% V doped TiO_2 (d).

The characteristic peaks from V_2O_5 were found in the XRD patterns of the 4.9 wt% V doped TiO_2. Rietveld refinement was carried out using the Fullprof program on the M-TiO_2 and the M-V doped TiO_2 samples. All the prepared materials consisted of anatase phase (major) and the Rietveld refinements are shown in Figure 2(a), 2(b), 2(c) and 2(d) respectively. The theoretical data are represented by the solid

line and the experimental points are expressed as dots (.). The difference between the experimental and the theoretical data is represented by the line at the bottom. The vertical lines (blue lines) represent the Bragg's allowed peaks. The results of the crystal system, cell parameters (a, b, c) and atomic position (x, y, z) are presented in Table 2.

Table 2 Crystal system, cell parameters (a, b, c), volume and atomic position (x,y,z) of M-TiO_2 and M-V doped TiO_2.

Prepared material	TiO_2 phase	Unit cell		Vol. ($Å^3$)	Atom	x	y	z	Rp	Rwp	χ^2
		a = b (Å)	c (Å)								
Pure TiO_2	Anatase (tetragonal, $I4_1/amd$)	3.7951	9.5316	137,28	Ti^{+4}	0.00	0.00	0.50	7.44	10.5	0.188
					O^{-2}	0.00	-0.50	0.5453			
2.3 wt% V doped TiO_2	Anatase (tetragonal, $I4_1/amd$)	3.7959	9.5384	137.44	Ti^{+4}	0.00	0.00	0.50	7.26	10.9	0.208
					O^{-2}	0.00	-0.50	0.5437			
3.3 wt% V doped TiO_2	Anatase (tetragonal, $I4_1/amd$)	3.7949	9.5361	137.33	Ti^{+4}	0.00	0.00	0.50	11.1	14.7	0.390
					O^{-2}	0.00	-0.50	0.5424			
4.9 wt% V doped TiO_2	Anatase (tetragonal, $I4_1/amd$)	3.7947	9.5368	137.33	Ti^{+4}	0.00	0.00	0.50	12.7	15.9	0.508
					O^{-2}	0.00	-0.50	0,5419			

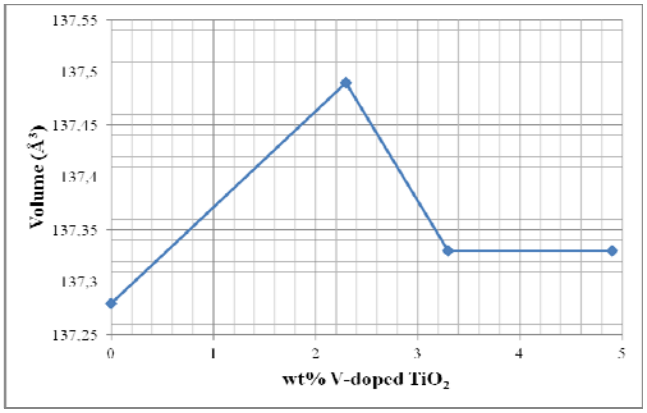

Figure 4 The influence of V doped TiO_2 on tetragonal lattice parameters (cell volume).

Figure 4 shows the influence of V doped TiO_2 on cell volume. In this case, the ionic radius of V^{5+} (0.054 nm) is compatible with that of Ti^{4+} (0.0605 nm) [31]. When the Ti^{4+} ion is replaced by the V^{5+} ion, the cell volume should become smaller, but in fact the cell volume becomes larger. This is because the insertion of oxygen (O^{2-}) to balance the cationic charge. Furthermore, the role of the ionic radius of V^{5+} (0.54 Å) is obvious on increasing the V-doped TiO_2 resulted in a decreased cell volume.

3.4 N_2 Adsorption/Desorption Measurement

The N_2 adsorption-desorption isotherms of representative prepared samples are displayed in Figure 5. According to the IUPAC classification, for pure TiO_2 (M-TiO_2) and 2.3 wt% vanadium-doped TiO_2 (Fig. 5a and 5b), the isotherms are of type IV, with a profile of type H2 hysteresis loops, while the 3.3 and 4.9 wt% vanadium doped TiO_2 both reflect isotherm type III. The isotherm type IV represents a capillary condensation phenomenon. The isotherm type is characteristic of a material that contains mesoporosity and high energy adsorption. Based on the type H2 hysteresis loop profile, the prepared materials have pores with narrow, wide sections and possible interconnecting channels. The isotherm type III explains the multilayer formation. This is characteristic of a material, that is not porous, or possibly macroporous, and has low energy adsorption [32,33].

Table 3 Surface Area, volume and pore size distribution of M-TiO_2 and M-V doped TiO_2 from nitrogen adsorption-desorption isotherm measurements.

Samples	Surface Area BET (S_{BET}) (m^2/g)	t-Plot Method			Pore Volume at $P/P_o \approx 0.99$ (cm^3/g)	Pore Size (nm) BJH_{ads}
		External Surface Area (m^2/g)	Micropore Volume (cm^3/g)	Micropore Area (m^2/g)		
Pure TiO_2	46	46	-	-	0.2565	18.45
2.3 wt% V doped TiO_2	40	39	0.00044	1	0.1738	15.46
3.3 wt% V doped TiO_2	23	22	0.00063	1	0.1729	28.72
4.9 wt% V doped TiO_2	17	10	0.00365	7	0.1289	41.20

The surface area, volume and pore size distribution of the prepared samples are summarized in Table 3. From the table, it can be seen that the concentration of V in the M-V doped TiO_2 increased while the BET surface area and mean pore size decreased with smallest surface area 17 m^2/g, which corresponds to a mean porous size of 41.20 nm in the 4.9 wt% V doped TiO_2. The BET surface area of the M-TiO_2 exhibited a maximum surface area of 46 m^2/g, corresponding to a mean porous size of 18.45 nm calculated by the $BJH_{ads.}$ method.

The pore size distribution curve was calculated from the adsorption-desorption isotherms by the procedure developed by Barrett, Joyner and Halenda (BJH). Figure 3(b)-3(d) (inset) depicts the pore size distribution of the M-TiO_2 and the M-V doped TiO_2 calculated by the BJH_{ads} method. The BJH adsorption-desorption analyses show that the prepared materials exhibited mesoporous material. The results of the BJH-adsorption analysis showed that the M-TiO_2 had a pore size of 18.45 nm, while the 2.3, 3.3, 4.9 wt% V doped TiO_2 had pore sizes of 15.46, 28.72,

41.20 nm, respectively. The pore sizes of the M-TiO_2 and the M-V doped TiO_2 are presented in Table 3.

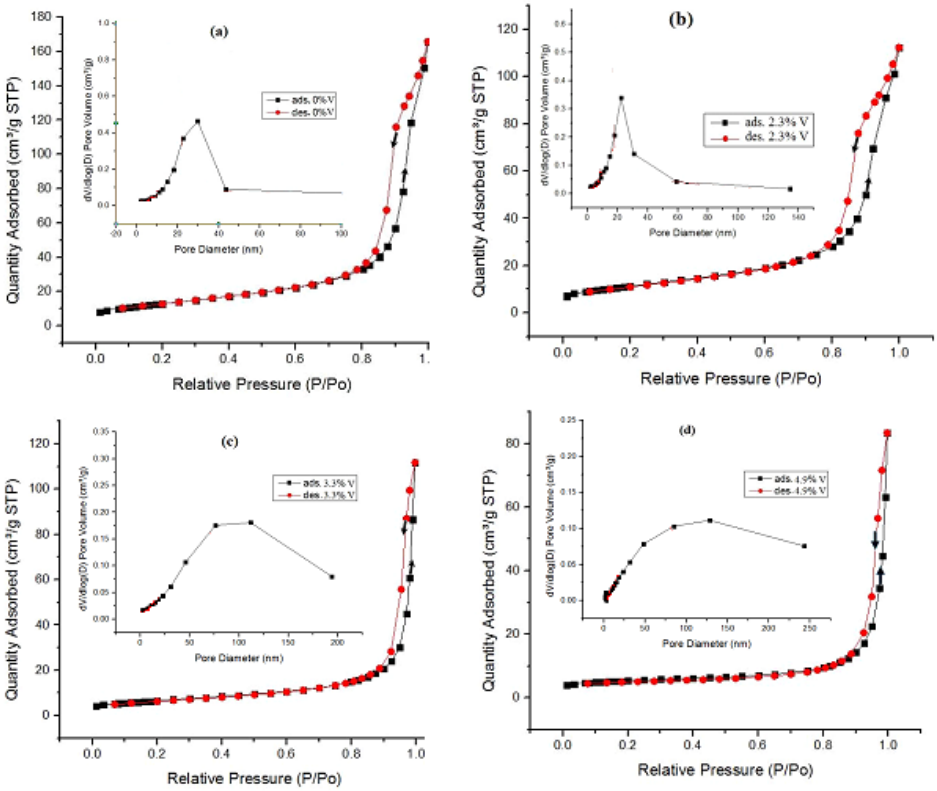

Figure 5 Nitrogen adsorption-desorption isotherms of M-TiO_2 (a), 2.3 wt% V doped TiO_2 (b), 3.3 wt% V doped TiO_2 (c), and 4.9 wt% V doped TiO_2 (d) (Inset: pore size distribution of the prepared samples from the adsorption isotherm measurements).

4 Conclusions

Mesoporous-TiO_2 (M-TiO_2) and mesoporous vanadium-doped TiO_2 (M-V doped doped TiO_2) at 2.3, 3.3 and 4.9 wt% vanadium-doped TiO_2, were successfully synthesized via reflux technique. All mesoporous vanadium-doped TiO_2 (M-V doped TiO_2) powders performed in a highly transparent mode in the visible region at 554 nm (E_g = 2.24 eV) and 588 nm E_g = 2.12 eV) for the 3.3 and 4.9 wt% V doped TiO_2, respectively. All the prepared mesoporous materials were in anatase phase (tetragonal, $I4_1/amd$). The isotherm type of the pure TiO_2 (M-TiO_2) and the 2.3 wt% vanadium-doped TiO_2 were of type IV with a profile of type H2 hysteresis loops, while the 3.3 and 4.9 wt% vanadium-doped TiO_2 reflected isotherm type III.

The smallest pore size of 18.45 nm was obtained for pure TiO_2 (M-TiO_2), while the largest pore size of 41.20 nm was obtained for 4.9 wt% vanadium-doped TiO_2 (M-V doped TiO_2).

Acknowledgements

The research was funded by the Directorate General of Higher Education, Ministry of Education and Culture, Republic of Indonesia based on PUPT 2014 Grant, No. 230/UPT-BOPTN/UN34.21/2014.

References

[1] Dai, Q., Zhang, Z., He, N., Li, P. & Yuan, C., *Preparation and Characterization of Mesostructured Titanium Dioxide and Its Application as a Photocatalyst for the Wastewater Treatment,* Materials Science and Engineering*,* **C8-9**, pp. 417-423, 1999.

[2] Awati, P.S., Awate, S.V., Shah, P.P. & Ramaswamy, V., *Photocatalytic Decomposition of Methylene Blue Using Nanocrystalline Anatase Titania Prepared by Ultrasonic Technique,* Catalysis Communications, **4**(8), pp. 393-400, 2003.

[3] Dwivedi, C., Dutta, V., Chandiran, A.K., Nazeeruddin, M.K. & Grätzel, M., *Anatase TiO_2 Hollow Microspheres Fabricated by Continuous Spray Pyrolysis as a Scattering Layer in Dye-Sensitised Solar Cells*, Energy Procedia, **33**, pp. 223-227, 2013.

[4] Grätzel, M. *Solar Energy Conversion by Dye-Sensitized Photovoltaic Cells*. Inorganic Chemistry, **44**, pp. 6841-6851, 2005.

[5] Ashkarran, A.A. & Mohammadizadeh, M.R. *Superhydrophilicity of TiO_2 Thin Films Using $TiCl_4$ as a Precursor*, Materials Research Bulletin, **43**, pp. 522-530, 2008.

[6] Masuda, Y. & Kato, K., *Liquid-Phase Patterning and Microstructure of Anatase TiO_2 Films on SnO_2:F Substrates Using Superhydrophilic Surface,* Chemistry of Material*,* **20**, pp. 1057-1063, 2008.

[7] Maness, P.C., Smolinski, S., Blake, D.M., Huang, Z., Wolfrum, E.J. & Jacoby, W.A., *Bactericidal Activity of Photocatalytic TiO_2 Reaction: Toward and Understanding of Its Killing Mechanism, Applied and Environmental*, Microbiology, **65**(9), pp. 4094-4098, 1999.

[8] Huang, Z., Maness, P.C., Blake, D.M., Wolfrum, E.J., Smolinski, S. & Jacoby, W.A., *Bactericidal Mode of Titanium Dioxide Photocatalysis*, Journal of Photochemistry and Photobiology A: Chemistry, **130**, pp. 163-170, 2000.

[9] Yang, G., Jiang, Z., Shi, H., Xiao, T. & Yan, Z., *Preparation of Highly Visible-Light Active N-Doped TiO_2 Photocatalyst*, Journal of Materials Chemistry, **20**, pp. 5201-5309, 2010.

[10] Yang, J., Bai, H., Jiang, Q. & Lian, J., *Visible-Light Photocatalysis in Nitrogen–Carbon-Doped TiO_2 Films Obtained by Heating TiO_2 Gel–Film in an Ionized N_2 Gas*, Thin Solid Films, **516**(8), pp. 1736-1742, 2008.

[11] Nishikiori, H., Hayashibe, M. & Fujii, T., *Visible Light-Photocatalytic Activity of Sulfate-Doped Titanium Dioxide Prepared by the Sol−Gel Method*, Catalysts, **3**, pp. 363-377, 2013.

[12] Wang, H., Niu, J., Long, X. & He, Y., *Sonophotocatalitic Degradation of Methyl Orange by Nanosized Ag/TiO_2 Particles in Aqueous Solutions*, Ultrasonic Sonochemistry, **15**, pp. 386-392, 2008.

[13] Al-Hartomy, O.A., *Synthesis, Characterization, Photocatalytic and Photovoltaic Performance of Ag-Doped TiO_2 Loaded on The Pt–Carbon Spheres*, Materials Science in Semiconductor Processing, **27**, pp. 71-78, 2014.

[14] Liu, B., Wang, X., Cai, G., Wen, L., Song, Y. & Zhao, X., *Low Temperature Fabrication of V-Doped TiO_2 Nanoparticles, Structure and Photocatalytic Studies*, Journal of Hazardous Materials, **169**(1-3), pp.1112-1118, 2009.

[15] Tian, B., Li, C. & Zhang, J., *One-Step Preparation, Characterization and Visible-Light Photocatalytic Activity of Cr-doped TiO_2 with Anatase and Rutile Bicrystalline Phases*, Chemical Engineering Journal, **191**, pp. 402-409, 2012.

[16] Thuy, N.M., Van, D.Q. & Hai, L.T.H., *The Visible Light Activity of the TiO_2 and TiO_2:V^{4+} Photocatalyst*, Nanomaterials and Nanotechnology, **2**(14), pp. 1-8, 2012.

[17] Zhang, Z., Shao, C., Zhang, L., Li, X. & Liu, Y., *Electrospun Nanofibers of V-Doped TiO_2 with High Photocatalytic Activity*, Journal of Colloid Interface Science, **351**, pp. 57-52, 2010.

[18] Songara, S., Patra, M.K., Manoth, M., Saini, L., Gupta, V., Gowd, G.S., Vadera, S.R. & Kumar, N., *Synthesis and Studies on Photochromic Properties of Vanadium Doped TiO_2 Nanoparticles*, Journal of Photochemistry and Photobiology A: Chemistry, **209**(1), pp. 68-73, 2010.

[19] Yang, X., Cao, C., Hohn, K., Erickson, L., Maghirang, R., Hamal, D. & Klabunde, K. *Highly Visible-Light Active C- and V-Doped TiO_2 for Degradation of Acetaldehyde*, Journal of Catalysis, **252**(2), pp. 296-302, 2007.

[20] Bettinelli, M., Dallacasa, V., Falcomer, D., Fornasiero, P., Gombac, V., Montini, T., Roman, L., & Speghini, A. *Photocatalytic Activity of TiO_2 Doped with Boron and Vanadium*, Journal of Hazardous Materials, **146**, pp. 529-534, 2007.

[21] Tian, B., Li, C., Gu, F., Jiang, H., Hu, Y. & Zhang, J., *Flame Sprayed V-doped TiO_2 Nanoparticles with Enhanced Photocatalytic Activity under Visible Light Irradiation*, Chemical Engineering Journal, **151**(1-3), pp. 220-227, 2009.

[22] Li, Z., Ding, D. & Ning, C., *p-Type Hydrogen Sensing with Al- and V-Doped TiO_2 Nanostructures*, Nanoscale Research Letter, **8**(25), pp. 1-8, 2013.

[23] Li, L., Chen, S., Xu, L., Bai, Y., Nie, Z., Liu, H. & Qi, L., 2014. *Template-Free Synthesis of Uniform Mesoporous SnO_2 Nanospheres for Efficient Phosphopeptide Enrichment*, Journal of Materials Chemistry B, **2**, pp. 1121-1124, 2014.

[24] Lu, B., Li, Z. & Kawamoto, K., *Synthesis of Mesoporous Ceria without Template*, Materials Research Bulletin, **48**(7), pp. 2504-2510, 2013.

[25] Jolivet, J.P., Henry, M. & Livage, J., De la Solution a L'oxyde: Condensation des Cations en Solution Aqueuse, Chimie de Surface des Oxydes. Inter édition et CNRS édition, 1994.

[26] Rich, R.L., *Inorganic Reactions in Water*, Springer, 2006.

[27] Roisnel, T. & Ridriguez-Carvajal, J., *WinPLOTR a Graphic Tool for Powder Diffraction*, CNRS-Lab. de Chimie du Solide et Inorganique Moléculaire Université de Rennes, 2001.

[28] Brunauer, S., Emmett, P.H. & Teller, E., *Adsorption of Gases in Multimolecular Layers*, Journal of the American Chemical Society, **60**(2), pp. 309-319, 1938.

[29] Barrett, E.P., Joyner, L.G. & Halenda, P.P., *The Determination of Pore Volume and Area Distributions in Porous Substances. I. Computations from Nitrogen Isotherms,* Journal of the American Chemical Society, **3**(1), pp. 373-380, 1951.

[30] Feist, T. P. & Davies, P.K. *The Soft Chemical Synthesis of TiO_2(B) from Layered Titanates*, Journal of Solid State Chemistry, **101**, pp. 275-295, 1992.

[31] Fu, C., Huang, Z., Li, J. & Guo, D., *Microstructure and Ferroelectric Properties of $(Bi_{0.9}Ho_{0.1})_{3.999}Ti_{2.997}V_{0.003}O_{12}$ Thin Films Prepared by Sol-gel Method for Nonvolatile Memory*, Journal Material Science Technology, **26**(8), pp. 679-681, 2010.

[32] Lowell, S., Shields, J.E., Thomas, M.A. & Thommes, M., *Characterization of Porous Solids and Powders: Surface Area. Pore Size and Density*, Springer, 2006.

[33] Condon, J.B., *Surface Area and Porosity Determinations by Physisorption Measurements and Theory*, 1st ed., Elsevier, 2006.